AERODYNAMIC PERFORMANCE PREDICTION OF HORIZONTAL AXIS WIND TURBINES

D. R. Jeng, T. G. Keith and A. Aliakbarkhanafjeh

Department of Mechanical Engineering
The University of Toledo
2801 W. Bancroft Street
Toledo, Ohio 43606

ABSTRACT

The purpose of this work is to describe a new method for calculating the aerodynamic performance of horizontal axis wind turbines. The method, entitled the helical vortex method, directly calculates the local induced velocity due to helical vortices that originate at the rotor blade. Furthermore, the method does not require a specified circulation distribution.

Results of the method are compared to similiar results obtained from Wilson PROP code methods (Prandtl, Goldstein, NASA and no tip loss) as well as to existing experimental data taken from the NASA Mod-0 wind turbine. It is shown that results of the proposed method agree well with experimental values of the power output both near cut-in and at rated wind speeds. Further, it is found that the method does not experience some of the numerical difficulties encountered by the PROP code when run at low wind velocities.

INTRODUCTION

Recently there has been a renewed interest in wind turbines as a means of producing power. Considerable effort has been directed toward experimental and theoretical studies of wind turbine performance.

At present, the analytical method used in predicting aerodynamic wind turbine performance by the NASA Wind Energy research group utilizes a modified blade element theory [1] or Glauert vortex theory incorporated with Prandtl [2], Goldstein [3] and NASA [4] tip loss models. In the Glauert vortex theory, it is assumed that trailing vortices originate from the rotating blades and form a helical vortex system that passes down stream. This vortex system, in turn, induces velocities which alter the flow around the blade. However, in this method, the induced velocities are not determined directly due to the complexity of the method. Instead, an interference velocity is calculated as the induced velocity of this vortex system on any blade element. The calculation of these interference velocities is simplified by assuming that the rotor has an infinite number of blades. The latter assumption removes the complexity associated with the periodicity of the flow and permits momentum theory to be directly used to evaluate the interference velocities. However, for single and double bladed rotors, this assumption may be inadequate.

Consider a wind turbine, rotating with an angular velocity Ω about its horizontal axis of rotation, that is placed in a uniform stream of wind of velocity V_o parallel to the axis of rotation. The blade can be coned or tilted to an angle of ψ from the plane perpendicular to the axis of rotation. The velocity experienced by the typical blade is shown in Fig. 1. It can be seen from Fig. 1, that $V_o(1-a)\cos\psi$ is the wind free stream velocity minus the axial interference velocity normal to the blade surface. Further, $\Omega r\{1+a'\}\cos\psi$ is the relative velocity of blade to the air velocity and accordingly is the angular velocity of the blade section plus the rotational interference velocity. The factors, a and a' are the axial and the rotational interference factors respectively.

In order to evaluate the local drag force and torque, the interference factors a and a' must first be determined. However, before presenting the equations for determining a and a', it may be helpful to review the tip and hub losses for a blade. It should be anticipated that the flow around a rotor blade of finite length will be disturbed at the tip and root or hub of the blade. These disturbances are due to the fact that the difference of pressure between the upper and lower sides of the blade disappear along the blade span and must therefore diminish to zero toward the tip and hub. An approximate method of estimating the effect of these radial disturbances has been given by Prandtl [2]. Later, a more accurate solution to this problem was developed by Goldstein [3]. Introducing a reduction factor, F, to account for the fact that only a fraction of the air between successive vortex sheets of the slip stream receives the full effect of the motion of these sheets, into the momentum equation for the flow at radius r and then equating the differential drag and torque equations obtained respectively from momentum and blade element theories, permits the writing of equations which must be satisfied by a and a'. These equations may be written as:

$$\frac{a}{1-a} = \frac{\sigma_L(C_L\cos\phi + C_D\sin\phi)\cos^2\psi}{4\,F\,\sin^2\phi} \qquad (1)$$

and

$$\frac{a'}{1+a'} = \frac{\sigma_L(C_L\sin\phi - C_D\cos\phi)}{4\,F\,\sin\phi\,\cos\phi} \qquad (2)$$

Expressions for the reduction factor F can be found in [2,3]. The tip loss method which has been used by NASA is the so-called "effective radius model". Due to the radial flow near the boundary of the slipstream, there is a drop of circulation which can be represented by an equivalent rotor with an infinite number of blades

and with the same drag force but with a smaller radius R_e, i.e., an effective radius is defined as

$$R_e = B_o \cdot R \tag{3}$$

where B_o is a constant tip loss factor.

Wilson and Walker [4] developed a computer program called PROP to evaluate the solution of eqs. (1) and (2). A preassigned tip loss factor (F = 1, no tip loss) was used and an iteration procedure for determining $\underline{a}$ and $\underline{a}'$ for a given differential element was employed. Once $\underline{a}$ and $\underline{a}'$ were determined, torque, drag and power could all be calculated from the appropriate equations. However, the value of the axial interference factor $\underline{a}$ has a limit. For a positive axial velocity V_o, the induced axial velocity of out flow near the rotor with a coning angle ψ is (V_o a cosψ), thus, from vortex theory, the induced axial velocity in the ultimate slipstream will be ($2V_o$a cosψ). Therefore, the trailing velocity of air far behind the rotor is [V_o(1-2a)cosψ]. Equations (1) and (2) are based on the notion that the axial velocity at any location is unidirectional, and, therefore, the analysis is valid only if $a \leq \frac{1}{2}$. If the rotor absorbs all the energy, i.e., $V_2 = 0$, then $\underline{a}$ would have a maximum value of $\frac{1}{2}$. Unfortunately, by using the PROP code to calculate $\underline{a}$, under certain operating conditions, particularly for large tip speed ratios (small wind velocities), the local value of the axial interference factor can exceed this limiting value for all tip loss models. Therefore, the equations cease to be valid. It was also found that the PROP code generally underestimated the performance [5, 6]. Accordingly, it is the purpose of this paper to develop a computational method for predicting aerodynamic performance of a horizontal axis wind turbine that avoids these difficulties. In this method, the induced velocity is directly calculated by integration of Biot-Savart's law under the assumption that a filament of the trailing vortices is helical in nature, extends infinitely downstream of the rotor, and has constant pitch and diameter. Of primary importance, the method does not use interference factors.

The predicted performance of wind turbines obtained by use of the present technique will be compared with those obtained from the PROP code and with some experimental data obtained from the Mod-0 100 kw wind turbine operated by NASA - Lewis Research Center in Sandusky, Ohio.

ANALYSIS

General Assumptions and Discription of the Problem

Two major assumptions upon which the present analysis is based may be stated as follows:

1.) The trailing vortex system is helicoidal with constant pitch and diameter, and extends infinitely far downstream from the blade.

2.) The relative velocity of a blade element to the medium is identical to that in two-dimensional motion if reference is made to the relative velocity between the element and the medium.

Unlike Goldstein theory, the helical vortex assumption does not restrict the circulation distribution along the blade. In the Goldstein theory, an optimum circulation distribution was used that corresponded to a rigid helicoidal vortex system moving backward with constant velocity. However, in both theories, it is assumed that the slipstream expansion may be secondary and thus neglected.

The physical model of the problem is illustrated in Fig. 2. The coordinate system, which is shown in Fig. 3 was chosen such that the z coordinate is the distance measured from the rotor to a segment of the trailing vortex parallel to the axis of rotation of the rotor and that the r axis is along the blade. The conning angle of blade is ψ. The induced velocities are computed in terms of the coordinate system in Fig. 3 as will be demonstrated in the next section.

Calculation of Induced Velocity

Suppose that circulation at a particular span location, say r, of the blade is Γ. The circulation at a nearby point, say r + dr is

$$\Gamma + \frac{d\Gamma}{dr}\,dr \quad .$$

The difference in these circulation values i.e.,

$\frac{d\Gamma}{dr}\,dr$, according to Helmholtz theory, the strength of a vortex that will spring out from the blade element of dr to form the trailing vortex, Fig. 2. The induced velocity normal to the resultant velocity W at a point r' due to the helical vortex filament originating from each of the blades and extending to infinity is determined, via the Biot-Savart' law [7] by,

$$w_n(\xi) = \int_{\xi_{hub}}^{1} \frac{\frac{d\Gamma}{d\xi}\,d\xi}{4\pi R\cos\psi} \sum_{k=1}^{B} \int_{o}^{\infty} \frac{N_1 + N_2}{D_1^{3/2}\, D_2^{1/2}}\,d\theta \tag{4}$$

where $N_1 = (\xi - \xi'\cos\theta_k)\xi\xi'$

$N_2 = [\xi(\theta\sin\theta_k + \cos\theta_k) - \xi']\lambda_o^2\cos^2\psi$

$D_1 = \xi^2 + \xi'^2 - 2\xi\xi'\cos\theta_k + \theta^2\lambda_o^2\cos^2\psi$

$D_2 = \lambda_o^2\cos^2\psi + \xi'^2$

$\theta_k = \theta + \frac{2\pi(B-k)}{B}$

$\lambda_o = \frac{V_o}{\Omega R\cos\psi}$

$\xi = \frac{r}{R}$

$\xi' = \frac{r'}{R}$

An expression similar to eq. (4) was employed by Plencner [8] for studying propeller characteristics.

The integration with respect to θ in eq. (4) is an arduous task. Furthermore, the form of the expression, as it stands, is inconvenient for practical use because the integral becomes infinitely great at the point $\xi' = \xi$ and $\theta = 0$. Clearly, this feature unless properly handled can cause considerable errors when calculating the induced velocity.

Moriya [7] proposed a method to remedy the problem. In his method, he introduced a so-called induction factor I which is defined as

$$I(\xi,\xi',\lambda_o) = (\xi-\xi') \sum_{k=1}^{B} \int_o^{\infty} \frac{N_1 + N_2}{D_1^{3/2} D_2^{1/2}} \, d\theta \qquad (5)$$

With this factor, the singularity at $\xi = \xi'$ can be shown to reduce eq. (4) to

$$w_n = \int_{\xi_{hub}}^{1} \frac{\frac{d\Gamma}{d\xi} \, d\xi \quad I}{4\pi R \cos\lambda \quad (\xi-\xi')} \qquad (6)$$

It should be mentioned that the induction factor, which is a continuous function of λ_o, ξ and ξ', is simply the ratio of the normal induced velocity for a helical trailing vortex system to the normal induced velocity for a straight trailing vortex system of the same strength. At a point $\xi' = \xi$, the induction factor I has a value of unity. In the following, the induction factor will be determined by numerical integration using 24 terms of a Lagurre-Gaussian Quadrature [9].

Governing Equation Formulation

The governing equation used in this study can be established from the fact that if the blade section is set at a geometrical angle of attack, α_g, relative to the incoming wind velocity, W, as shown in Fig. 4, its setting relative to W is α_g diminished by the downwash angle, α_i. This relation may be written as

$$\alpha_g = \alpha_e - \alpha_i \qquad (7)$$

where

$$\alpha_i = \tan^{-1} \frac{w_n}{W}$$

and α_e is an effective angle of attack. The negative sign appearing in eq. (7) occurs because the induced angle of attack, α_i, is itself a negative number. The geometric angle of attack can be obtained from Fig. 4 as

$$\alpha_g = \tan^{-1} \frac{\lambda_o \cos\psi}{\xi'} - \beta \qquad (8)$$

where β is the pitch angle of the blade element at ξ'.

The induced angle of attack may be expanded in series form in terms of $\frac{w_n}{W}$. Moreover, because the value of $\frac{w_n}{W}$ is usually small, it may be assumed that

$$\alpha_i \cong \frac{w_n}{W} = \int_{\xi_{hub}}^{1} \frac{I(\xi,\xi',\lambda_o) \frac{d\Gamma}{d\xi} \, d\xi}{4\pi\Omega R^2 \cos^2\psi \, D_2^{\frac{1}{2}} \, (\xi - \xi')} \qquad (9)$$

The circulation function, Γ, may be expressed as a Fourier-Sine series satisfying the following boundary conditions

$$\Gamma(\xi = 1) = \Gamma(\xi_{hub}) = 0$$

An expression that meets these conditions may be written as

$$\Gamma(\xi) = \sum_{m=1}^{\infty} A_m \sin m\pi \left(\frac{\xi - \xi_{hub}}{1 - \xi_{hub}} \right) \qquad (10)$$

The relation between circulation and lift coefficient is given by the Kutta-Joukowski theorem for a two-dimensional airfoil as

$$\Gamma = \tfrac{1}{2} c W C_L \qquad (11)$$

where c is the chord length.

Using equations (5) and (7) through (11), the aerodynamic characteristics for a given blade element can be determined. The calculation involves an iteration process and requires that the series for Γ be truncated at N terms. A computer program has been developed for this iteration and proceeds according to the following logic:

1) Assume $\alpha_e = \alpha_g$ in the first iteration.

2) Find C_L from two-dimensional airfoil data such as that shown in Figs. (5) and (6). In the program, experimental data for C_L and C_D were curve fitted using polynomials and were stored in the program.

3) Calculate the local circulation $\Gamma(\xi)$ by employing eq. (11).

4) With the values of $\Gamma(\xi)$ known at each location ξ, the constant's, A_m, appearing in eq. (10) can be determined by solving a set of linear algebric equations.

5) Calculate local α_i by using eq. (9). This can be done by substituting eq. (10) into eq. (9) and integrating the resulting equation. However, in practice, the integral is broken into three separate integrals to remove the singularity as follows

$$\int_{\xi_{hub}}^{1} g(\xi)d\xi = \int_{\xi_{hub}}^{\xi'-\delta} g(\xi)d\xi + \int_{\xi'-\delta}^{\xi'+\delta} g(\xi)d\xi + \int_{\xi'+\delta}^{1} g(\xi)d\xi \qquad (12)$$

where δ is an arbitraily small number, say $\delta = 10^{-5}$.

The first and the last terms on the right hand side of eq. (12) can be evaluated by using standard numerical integration procedures. The second integral on right hand side of eq. (12) contains a singularity, but, it can be shown that its value is very small, $0(10^{-4})$, and, thus, may be ignored in the calculation.

6) Calculate a new $\alpha_e = \alpha_g + \alpha_i$.

7) Obtain C_L from two-dimensional data using newly calculated α_e.

8) Compare the current C_L to the previous value of C_L, and if equal, stop, otherwise repeat the iteration by returning to step 3.

Power, Torque and Drag on Wind Turbine

Once the iteration process is successfully terminated and the effective angle of attack distribution calculated, the rotor thrust, torque and power can be calculated respectively from the following equations

$$\frac{dT}{dr} = \tfrac{1}{2}\rho BcW^2(C_L\cos\phi+C_D\sin\phi)\cos\psi$$

$$\frac{dQ}{dr} = \tfrac{1}{2}\rho BcW^2(C_L\sin\phi-C_D\cos\phi)r\cos\psi$$

Integration yields

$$T = \int_{\xi_{hub}}^{1} (\tfrac{1}{2}\rho BcW^2)(C_L\cos\phi+C_D\sin\phi)R\cos\psi d\xi \qquad (13)$$

$$Q = \int_{\xi_{hub}}^{1} (\tfrac{1}{2}\rho BcW^2)(C_L\sin\phi-C_D\cos\phi)R^2\cos\psi \; d\xi \qquad (14)$$

$$P = \int_{\xi_{hub}}^{1} (\tfrac{1}{2}\rho BcW^2)(R^2\Omega\cos\psi)(C_L\sin\phi-C_D\cos\phi)\xi d\xi \qquad (15)$$

RESULTS AND DISCUSSION

The proposed method has been used to calculate performance of two-bladed wind turbines. The particular blade and operating conditions, listed in Table 1 and used in the calculations, correspond to those of NASA's Mod-0, 100kw large wind turbine located in Sandusky, Ohio. Further description of this facility may be found in [10].

A circulation distribution corresponding to the operating condition tabulated in Table 1 is plotted in Fig. 8. As one can see, it is quite irregular and departs greatly from an eliptical shape generally used in aerodynamic studies in which the distribution of circulation is unknown.

An empirical expression, taken from [11], was used in the calculations to compare predicted to recorded alternator power. This expression accounts for drive train losses and is given as

$$P_G = 0.95\ (P_R - 0.075\ P_E) \qquad (16)$$

in which:

P_G ; generated electrical power, kw

P_R ; power produced by rotor, kw

P_E ; rated electrical power, kw (100 kw).

Predicted alternator power is plotted against wind speed in Fig. 9. Also shown are corresponding theoretical results obtained by using the PROP computer code and existing experimental data [12].

From these figures, it can be seen that there is a closer correlation between the values predicted by the present method and the experimental data than there is with the four PROP code methods of predictions. It is generally known that PROP code models underestimate performance compared with experimental data [5, 11, 13]. However, our results are 10 to 15% higher than are PROP code values for wind speeds ranging from 8 to 20 mph. There is excellent agreement between our data and the experimental values. Our data predicts a "cut-in" wind speed of 8 mph which agrees with the actual value reported in [5]. It is known that the "cut-in" speed is not predicted accurately by any of the methods found in the PROP code.

Other calculations have been made for the MOD-1 wind turbine (2MW). The operating conditions and the input data for these calculations are listed in Table II. The airfoil used for the blade construction is an NACA 4418 with a "half rough" surface condition and a variable twist angle along the blade span.

The chord and twist angle are tabulated in Table III.

The power coefficient C_p vs. tip speed ratio for MOD-1 is presented in Fig. 10. As can be seen, the results obtained from the PROP code are unlikely as the power coefficient has a saddle-like distribution. On the other hand, our results do not exhibit this behavior. It is believed that incorrect handling of the interference factors is the source of the difficulty.

ACKNOWLEDGEMENTS

The research project was sponsered by NASA Wind Energy Research Program under the contract number NCC3-5.

REFERENCES

[1] W. F. Durand, (Ed.) "Aerodynamic Theory" Chap. VII, Sec. 4, pp. 169-360.

[2] L. Prandtl, "Application of Modern Hydrodynamics to Aeronautics", NASA Report 116, 1921.

[3] S. Goldstein, "On the Vortex Theory of Screw Propellers", Proceeding of the Royal Society of London, Series A, 123, 1923.

[4] R. E. Wilson and S. N. Walker, "A Fortran Program for the Determination of Performance, Loads, and Stability Derivatives of Wind Tubelnes", Department of Mechanical Engineering Oregon State University, Corvallis, Oregon, Oct. 1974.

[5] T. Richards, "Mod-0 Performance" NASA Lewis Research Center, Cleveland, Ohio, Wind Energy Project PIR No. 11, 1977.

[6] L. Viterna, "An Improved Aerodynamic Model for Wind Turbines", NASA Lewis Research Center, Cleveland, Ohio, Wind Energy Project PIR 144 1980.

[7] T. Moriya, "Selected Scientific and Technical Papers", University of Tokyo, Tokyo, Japan 1959.

[8] R. M. Plencner, "Numerical Analysis of Subsonic Propellers", Master Thesis of Aeronautical and Astronautical Engineering, University of Illinois at Urbana-Champaign, 1975.

[9] Shao, Chen, Frank, "Tables of Zeros and Caussian Weights of Certain Associated Laguerre Polynomials and Related Generalized Hermite Polynomials", IBM Technical Report TR00.1100, March 1964.

[10] R. L. Thomas and T. R. Richards, "ERDA/NASA 100 kw Mod-0 Wind Turbine Operations and Performance", ERDA/NASA/1028-7719, NASA TM-73825.

[11] L. Viterna, "Mod-0 Utility Pole Blade Performance", NASA Lewis Center, Cleveland, Ohio Wind Energy Project PIR 109, 1979.

[12] H. Neustadter and R. Wolf, "Mod-0 Hard and Soft Tower; Utility Pole Blades; Power, Flap Bending, Chord Bending and Horizontal Acceleration", NASA Lewis Research Center, Cleveland Ohio, Wind Energy Project PIR 106, 1979.

[13] L. Viterna, "An Improved Aerodynamic Model for Wind Turbines", NASA Lewis Research Center, Cleveland, Ohio, Wind Energy Project PIR 144, 1980.

NOMENCLATURE

a	axial interference factor
a'	rotational interference factor
B	number of blade
c	chord
C_D	drag coefficient
C_L	lift coefficient
C_P	power coefficient
L	lift
P	power
Q	torque
Q_c	torque coefficient
r	distance along the blade
r_L	r cos ψ
R	radius of rotor
Re	effective radius
T	thrust
V_o	wind velocity
w_n	normal induced velocity
W	vector sum of rotational and wind velocity
W'	vector sum of W and w_n
z	rearward distance from the rotor
α	angle of attack
α_e	effective angle of attack
α_g	geometric angle of attack
α_i	induced angle of attack
β	pitch angle
Γ	circulation
ρ	density
σ_L	solidity = $\frac{BC}{2 r_L}$
ψ	corning angle
Ω	rotational speed of blade

Table I - Operating Condition of the Utility Pole Wind Turbine

Root/Tip Chord	6.25/2.08
Chord Distribution	see Fig. 7
Percent Root Cut	23%
Blade Radius R, ft	62.5
Conning Angle, deg.	3.8
Solidity	0.033
Thickness to Chord Ratio	.24
Airfoil	NASA 230-24
Pitch Angle	0
Airfoil Surface	Rib Stitched, Fiberglass Cloth (half rough)
Operating RPM	32 and 33 rpm for 2 blade
Twist Angle	0

Table II - Input Data and Operating Condition for MOD-1 Wind Turbine (2MW)

Root/Tip Chord	12/2.82
Blade Radius R, ft.	100.8
Hub Radius	9.75
Percent Root Cut	10%
Conning Angle, deg.	9
No. of Blade	2
Airfoil	NASA 4418 (half rough)
Pitch Angle	0
Operating RPM	34.7
Solidity	0.042

Table III - Chord and Twist Angle

r/R	Chord ft.	Twist Angle degree
1	2.82	-3
.9	3.9	-1.85
.8	5.0	-0.62
.7	5.95	0.62
.6	6.95	1.85
.5	8.0	3.0
.4	9.0	4.28
.3	10.03	5.5
.2	11.03	6.69
.1	12.0	8.0

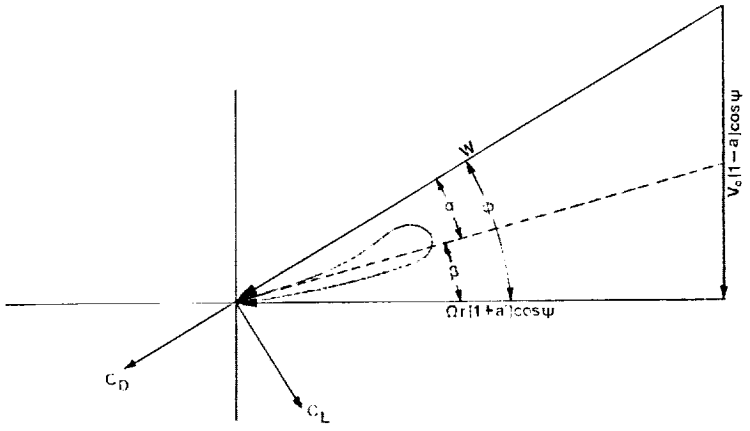

Fig. 1 - Force and velocity diagram for Glauert vortex theory.

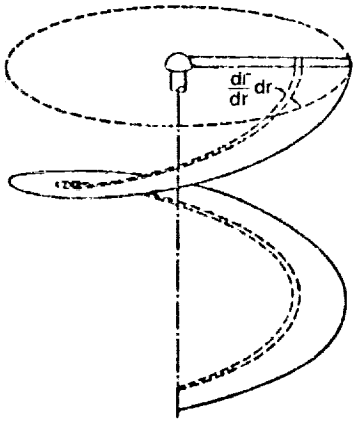

Fig. 2 - Physical model of the problem.

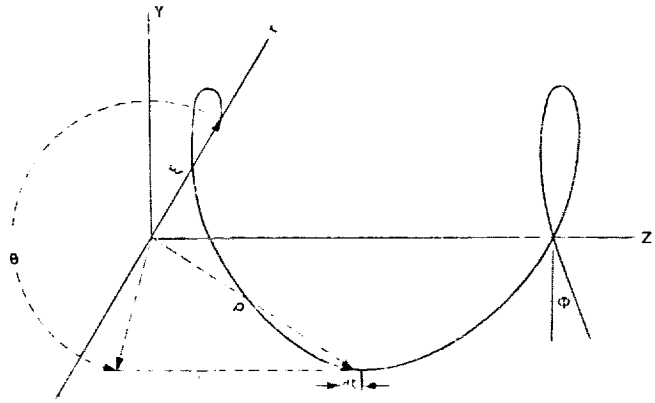

Fig. 3 - Helical vortex geometry and coordinate system.

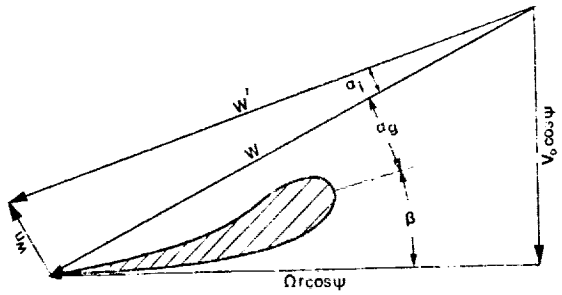

Fig. 4 - Velocity diagram showing the effect of induced velocity.

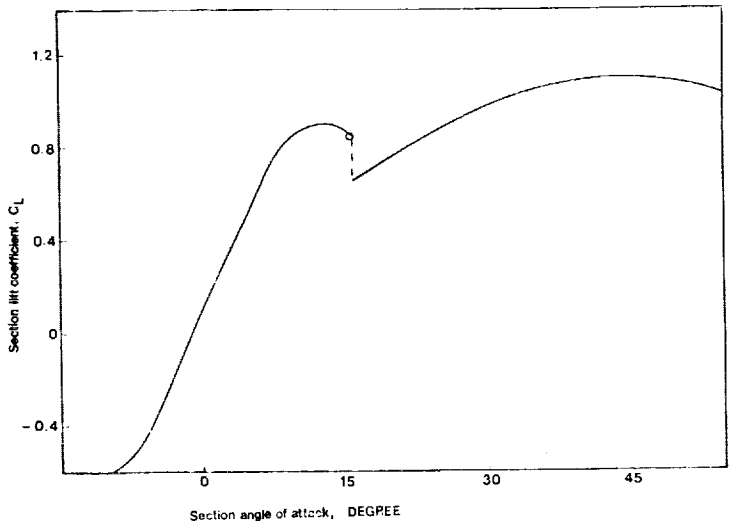

Fig. 5 - Lift coefficient vs. angle of attack for a half rough 23024 airfoil.

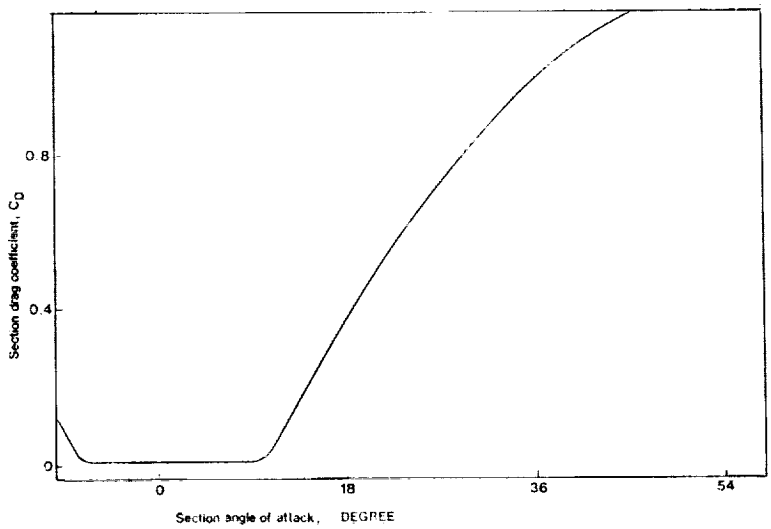

Fig. 6 - Drag coefficient vs. angle of attack for a half rough 23024 airfoil.

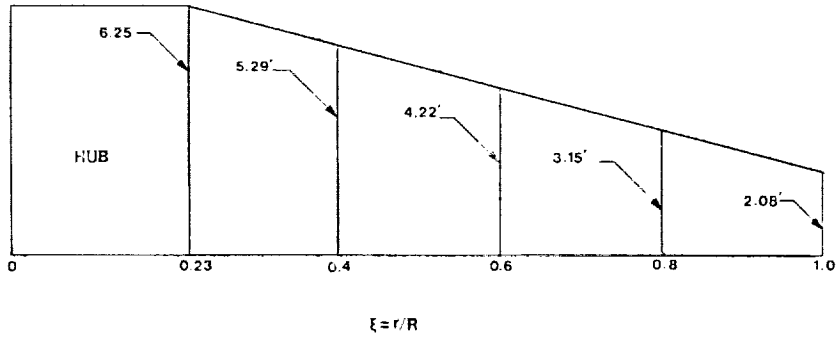

Fig. 7 - Chord distribution along the blade.

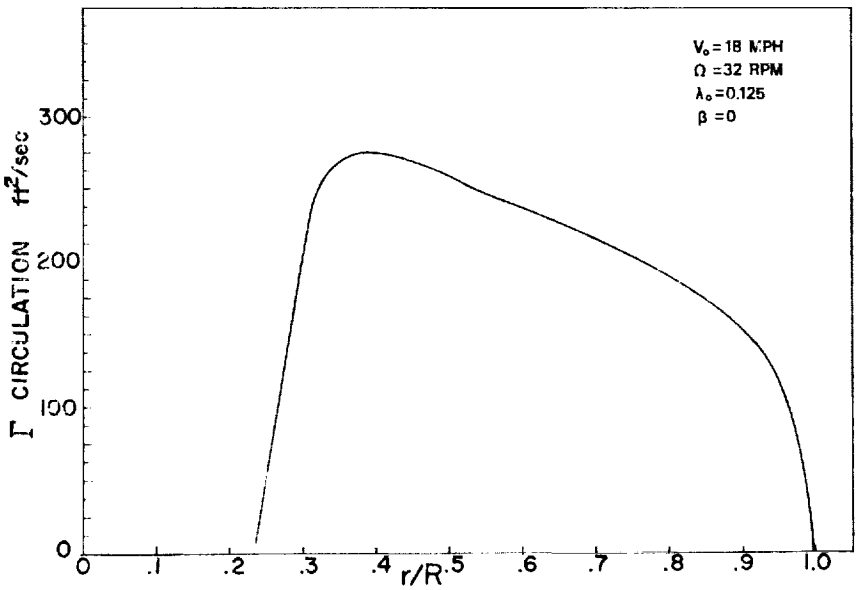

Fig. 8 - Circulation Distribution.

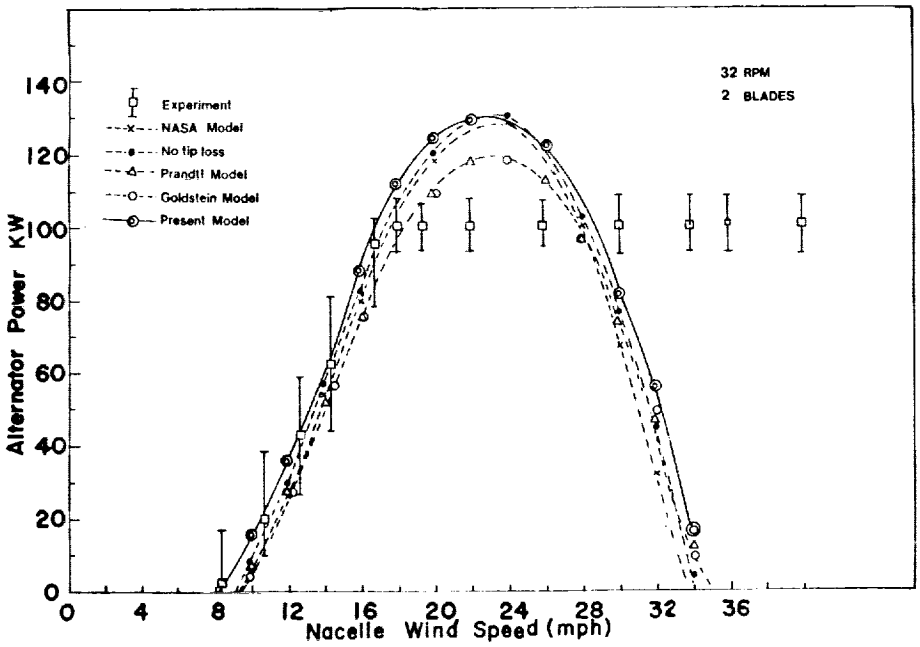

Fig. 9 - Alternator power vs. wind speed; zero pitch angle.

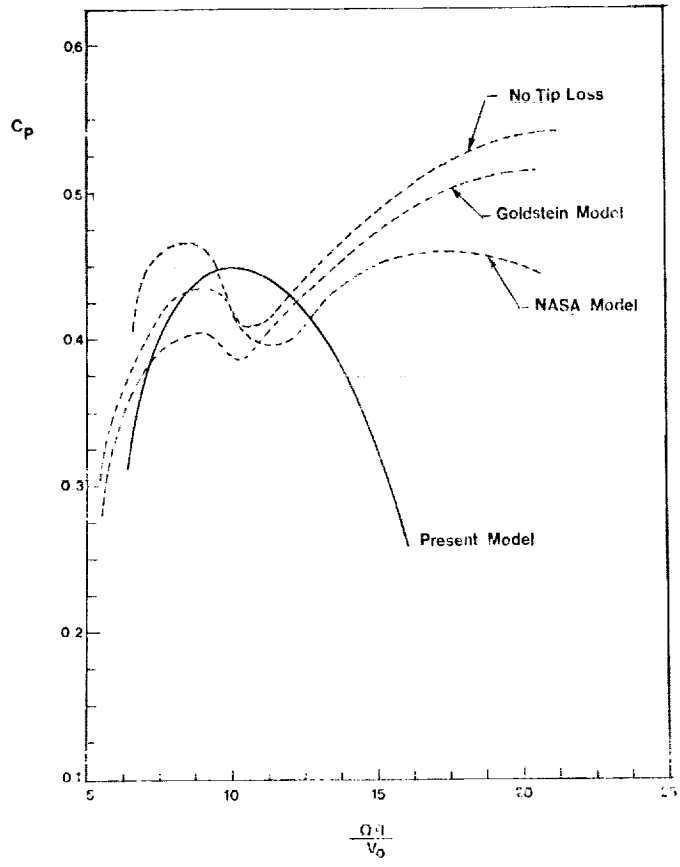

Fig. 10 - Cp vs. tip speed ratio, MOD-1 (NASA 4418 airfoil).

QUESTIONS AND ANSWERS

D. Jeng

From: Anonymous

Q: Can you comment on actual power being higher than predicted at high wind speed?

A: *Comparison between experimental and theoretical values is valid only between wind speeds of 8 mph to 18 mph. When the wind turbine reaches the rated power of 100 kW. Because the blade geometry for the theoretical calculation was not changed, the actual power and predicted power cannot be compared for wind speeds which exceed the rated value of 18 mph (Fig. 9).*

From: Anonymous

Q: Can any conclusion about aerodynamic correlation be drawn from cut in speed results which are largely dependent on mechanical friction and may vary from season to season?

A: *To obtain alternator power, the rotor power values were corrected for drive train losses by an empirical equation applicable for the MOD-0 wind turbine and given in the text. It is assumed that the power loss due to friction for this particular machine is 7.5 kW which is constant. By comparing the cut-in speed, we can compare the actual rotor power (alternator power is zero) and the predicted rotor power at the lowest wind speed.*